XFEM 2011
II European Conference on eXtended Finite Element
Cardiff University, United Kingdom
Cardiff, June 29-30 July 1, 2011

Self-affine Scaling of Simulated Intergranular Cracks in Brittle Polycrystals

Z. Shabir[1], L. Ponson[2], A. Simone[1]

[1] *Faculty of Civil Engineering and Geosciences, Delft University of Technology*
P.O. Box 5048, 2600 GA Delft, The Netherlands, {z.shabir, a.simone}@tudelft.nl
[2] *CNRS and Université Paris 06, UMR 7190, Institut Jean Le Rond d'Alembert*
F-75005 Paris, France, ponson@dalembert.upmc.fr

1 Introduction and method of analysis

The statistical analysis of fracture surfaces is a valuable tool for understanding failure mechanisms in engineering materials [1]. Self affinity of the fracture surfaces has been established through a significant amount of experimental work [2–4] and is described by the scaling relation $h(\lambda x) = \lambda^{\zeta} h(x)$, where $h(x)$ is the height distribution of a crack profile, λ is a scaling factor, and ζ is a parameter, known as Hurst or roughness exponent, which characterizes the roughness of the cracked surface. The Hurst exponent ζ remains invariant under a scale transformation. With reference to the experimental characterization of fracture in 3D brittle materials, Milman et al. [5] found a Hurst exponent $\zeta_{3D} = 0.4 \pm 0.15$ for the fracture surface in tungsten single crystals and highly oriented pyrolitic graphite. For materials exhibiting intergranular brittle fracture, Boffa et al. [6] reported an exponent equal to 0.5. Ponson et al. [7] have observed the self-affine properties of cracked surfaces of compacted brittle granular materials and reported $\zeta_{3D} = 0.46 \pm 0.05$. From the theoretical side, fracture surfaces have been modeled as the trace left by the crack front as it propagates through an elastic solids with random spatial fluctuations of fracture energy, leading to a value of roughness exponent $\zeta_{3D}^{th} = 0.39$ close to the experimental values [8, 9]. For crack propagation in 2D systems, the value of the roughness exponent is a priori different, since failure consists now of the propagation of the crack tip in a 2D plane, contrary to the motion of the crack line in 3D settings [10]. In these geometries, experimental studies have led to values close to $\zeta_{2D} \simeq 0.6 - 0.7$ (see *e.g.* Ref. [11]), but have been mainly devoted to systems with rather complex microscopic failure mechanisms such as viscoelasticity and microcracking. As a result, the connexion with the theoretical models issued from Fracture Mechanics that predict rather smaller values ($\zeta_{2D}^{th} \leq 0.50$) [12, 13] is not clear.

This study has been designed in order (i) to clarify the discrepancy between theory and experiments on the morphology of crack profiles in 2D setting, and (ii) to understand the role played by the microstructure of polycrystalline materials on their fracture surfaces during brittle and intergranular failure. For these reasons, we have simulated intergranular cracks in brittle polycrystalline materials. Intergranular crack paths are obtained with a Generalized Finite Element Method (GFEM) for polycrystals [14]. This method provides an accurate description of the stress field in a polycrystalline material and yields reliable crack paths [15]. In our approach, a polycrystal is obtained by the superposition of a polycrystalline topology on a simple background finite element mesh which does not need to conform to the local features of the topology. This superposition is automatically handled using the partition of unity property of finite element shape functions hence automating the mesh generation stage. A sequential polycrystalline analysis approach is used to handle our large simulations as discussed in Section 3. Resulting crack profiles are analyzed using the height-height correlation function in section 4. The estimated value of the Hurst exponent is compared with recent experimental and theoretical findings.

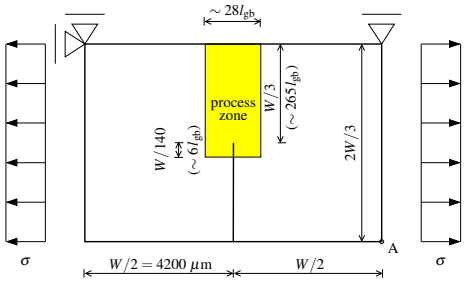

Figure 1: Geometry and boundary conditions for the notched specimen employed in the simulations.

2 Test setup and material

The geometry and boundary conditions of the test setup are reported in Figure 1. The material parameters are taken to be representative of an average polycrystalline alumina, Al_2O_3, with Young's modulus $E =$ 384.6 GPa and Poisson's ratio $\nu = 0.237$. Plane strain analyses are performed under the assumption of small elastic strains and rotations considering quasi-static loading conditions. A centroidal Voronoi tessellation algorithm is used to generate 18 different topologies of 3140 grains each. These topologies are embedded in the process zone shown in Figure 1. The average grain size is $\approx 20\ \mu$m, with an average grain boundary length $l_{gb} \approx 10.62\ \mu$m. The linear elastic isotropic grains are separated from each other by means of cohesive grain boundaries which follow the Xu-Needleman cohesive law [16] incorporating secant unloading and reloading behavior. According to Shabir et al. [15], intergranular crack paths in brittle polycrystals are not influenced by key cohesive law parameters. Following this argument, the mode-I fracture energy G_{Ic} and the maximum normal cohesive strength σ_{max} are set equal to 39.6 Jm^{-2} and 0.6 GPa, respectively. With this set of cohesive law parameters, relatively coarse meshes can resolve the cohesive law along grain boundaries.

3 Sequential polycrystalline analysis

Crack paths are generated using a sequential polycrystalline analysis approach. With this approach, large crack propagation simulations can be carried on by considering a suitable number of cheaper sub-simulations with a considerable saving in terms of computational effort. A typical example is shown in Figure 2(a) with the first and last simulations reported in Figures 2(b) and (c), respectively. The blue boxes in these figures show the area where the crack is allowed to propagate within a sub-simulation. Each box is termed "process window". Two different levels of mesh refinement are used in each of these sub-simulations. The mesh in the process window is characterized by a level of refinement according to [15], whereas the region outside is refined by providing at least two elements along each grain boundary. When a crack touches the end of a process window, the simulation is stopped and the resulting crack profile is saved. The next sub-simulation is launched considering the saved crack profile from the previous simulation. A new crack tip is defined by reducing the length of the loaded crack profile such that the new tip is now at a position where the cohesive strength of the previous simulation would be negligible. In other words, we make sure that nonlinear processes are accurately captured by enclosing nonlinear regions with a process window. We have found that an overlap of $\approx 2.5 l_{gb}$ between two consecutive process windows satisfies this requirement with the current choice of cohesive law and parameters. Unlike classical adaptive refinement approaches, the only information that is transferred from simulation to simulation is the crack path.

We have compared our approach with a monolithic approach on a series of polycrystalline topologies and the resulting crack paths are identical. Moreover, with reference to the load-displacement curves, if all the curves obtained with the sequential analysis approach were joined together by removing the pre-peak branch of each sub-simulation except the first one, then the resulting curve would follow the

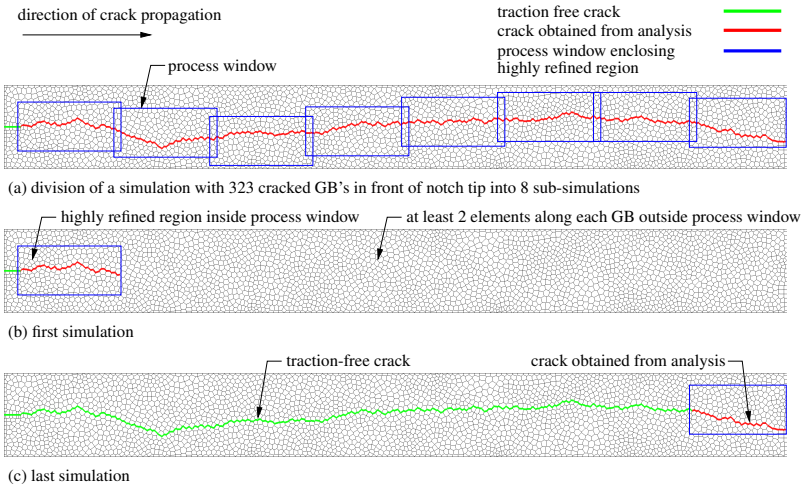

Figure 2: Sequential polycrystalline analysis of a 3140-grain topology.

curve obtained with the monolithic approach very closely. As for the stress field, we could hardly find any difference.

4 Roughness characterization of the crack profiles

In order to characterize the statistical properties of the numerical fracture surfaces, we analyze 18 crack profiles characterized by ≈ 315 cracked grain boundaries obtained from 3140-grain samples —each sample corresponds here to different polycrystalline arrangements. We use the height-height correlation function defined as $\Delta h(\delta x) = \langle [h(x+\delta x) - h(x)]^2 \rangle_x^{1/2}$. Its variations are represented in Figure 3 in logarithmic scales. It follows a power-law, reminiscent of self-affine properties, characterized by the roughness exponent $\zeta \simeq 0.50$ in a rather large range of length scales, from the typical length of the grain boundaries (≈ 10 μm) to a fraction of the system size ($\xi = 800$ μm $\approx L_f/4$, where L_f is the fracture ligament length equal to $W/3$).
Such a value of the Hurst exponent is smaller than the experimental findings $\zeta_{2D} \simeq 0.6 - 0.7$ obtained in 2D materials such as paper sheets [11]. However, such materials are known to give rise to microcracking and damage ahead of the main crack during crack propagation while in the polycrystalline materials considered here failure mechanisms are perfectly brittle. As a result, those two different values of roughness exponent are in rather good agreement with the scenario proposed in Ref. [17] where brittle and damage failure of disordered 2D materials are expected to give rise to $\zeta_{2D}^{th} \leq 0.5$ and $\zeta_{2D}^{th} > 0.5$, respectively. Why brittle intergranular failure of polycrystalline materials studied here gives rise to $\zeta \simeq 0.50$, and to which extent our findings can be understood within the framework developed in Refs. [12, 17] are still open questions.

Acknowledgements

This research is supported by the Higher Education Commission, Pakistan.

References

[1] E. Bouchaud. Scaling properties of cracks. *Journal of Physics: Condensed Matter*, 9(21):4319–4344, 1997.

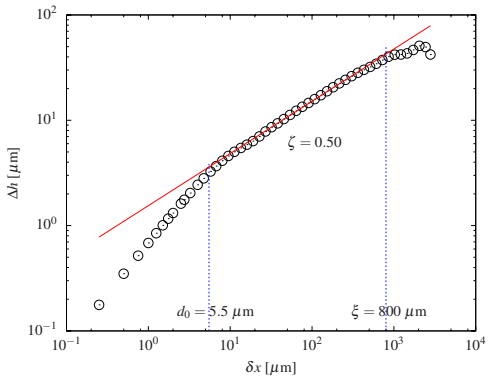

Figure 3: Hurst exponent ζ estimated on crack profiles obtained from 18 3140-grain topologies.

[2] B. B. Mandelbrot, D. E. Passoja, and A. J. Paullay. Fractal character of fracture surfaces of metals. *Nature*, 308(19):721–722, 1984.

[3] K. J. Måløy, A. Hansen, E. L. Hinrichsen, and S. Roux. Experimental measurements of the roughness of brittle cracks. *Physical Review Letters*, 68(2):213–215, 1992.

[4] L. Ponson, D. Bonamy, and E. Bouchaud. Two-dimensional scaling properties of experimental fracture surfaces. *Physical Review Letters*, 96(3):035506, 2006.

[5] V. Yu. Milman, R. Blumenfeld, N. A. Stelmashenko, and R. C. Ball. Comment on "experimental measurements of the roughness of brittle cracks". *Physical Review Letters*, 71(1):204, 1993.

[6] J. M. Boffa, C. Allain, and J. P. Hulin. Experimental analysis of fracture rugosity in granular and compact rocks. *The European Physical Journal - Applied Physics*, 2(3):281–289, 1998.

[7] L. Ponson, H. Auradou, M. Pessel, V. Lazarus, and J. P. Hulin. Failure mechanisms and surface roughness statistics of fractured fontainebleau sandstone. *Physical Review E*, 76(3):036108, 2007.

[8] D. Bonamy, L. Ponson, S. Prades, E. Bouchaud, and C.Guillot. Scaling exponents for fracture surfaces in homogeneous glass and glassy ceramics. *Physical Review Letters*, 97:135504, 2006.

[9] L. Ponson. Crack propagation in disordered materials: How to decipher fracture surfaces. *Annales de Physique*, 32(1):1–128, 2007.

[10] D. Bonamy and E. Bouchaud. Failure of heterogeneous materials: A dynamic phase transition? *Physics Reports*, 498(11):1–44, 2011.

[11] M. Mallick, P. P. Cortet, S. Santucci, S. G. Roux, and L.Vanel. Discrepancy between sub-critical and fast rupture roughness: A cumulant analysis. *Physical Review Letters*, 98:255502, 2007.

[12] E. Katzav, M. Adda-Bedia, and B. Derrida. Fracture surfaces of heterogeneous materials: A 2d solvable model. *Europhysics Letters*, 78(4):46006, 2007.

[13] I. Ben-Dayan, E. Bouchbinder, and I. Procaccia. Random and correlated roughening in slow fracture by damage nucleation. *Physical Review E*, 74:146102, 2006.

[14] A. Simone, C. A. Duarte, and E. Van der Giessen. A Generalized Finite Element Method for polycrystals with discontinuous grain boundaries. *International Journal for Numerical Methods in Engineering*, 67(8):1122–1145, 2006.

[15] Z. Shabir, E. Van der Giessen, C. A. Duarte, and A. Simone. The role of cohesive properties on intergranular crack propagation in brittle polycrystals. *Modelling and Simulation in Materials Science and Engineering*, 19(3):035006, 2011.

[16] X.-P. Xu and A. Needleman. Numerical simulations of fast crack growth in brittle solids. *Journal of the Mechanics and Physics of Solids*, 42(9):1397–1434, 1994.

[17] E. Bouchbinder, J. Mathiesen, and I. Procaccia. Roughening of fracture surfaces: The role of plastic deformation. *Physical Review Letters*, 92:245505, 2004.